

E-ISSN: 2708-3977

P-ISSN: 2708-3969

Impact Factor (RJIF): 5.73

IJEDC 2026; 7(1): 34-40

© 2026 IJEDC

[www.datacomjournal.com](http://www.datacomjournal.com)

Received: 22-10-2025

Accepted: 26-11-2025

**Michael James Robertson**  
Department of Electrical and  
Computer Engineering,  
University of Toronto,  
Toronto, Canada

**Jennifer Anne MacLeod**  
Department of Electrical and  
Computer Engineering,  
University of Toronto,  
Toronto, Canada

**Daniel Christopher Wong**  
Department of Electrical and  
Computer Engineering,  
University of Toronto,  
Toronto, Canada

**Laura Elizabeth Chen**  
Department of Electrical and  
Computer Engineering,  
University of Toronto,  
Toronto, Canada

**Correspondence**  
**Michael James Robertson**  
Department of Electrical and  
Computer Engineering,  
University of Toronto,  
Toronto, Canada

## Thermal management approaches for power electronic semiconductors in cold climate applications

**Michael James Robertson, Jennifer Anne MacLeod, Daniel Christopher Wong and Laura Elizabeth Chen**

**DOI:** <https://www.doi.org/10.22271/27083969.2026.v7.i1a.93>

### Abstract

Power electronic converters operating in northern Canadian environments face thermal management challenges spanning extreme temperature ranges from winter lows approaching -40°C to summer peaks exceeding 35 °C. This research evaluated thermal performance of four semiconductor device technologies across multiple cooling approaches under conditions representative of year-round operation in continental Canadian climates. Laboratory testing at the University of Toronto Power Electronics Research Centre between January 2023 and October 2023 characterized junction temperature distributions, thermal resistance values, and reliability under accelerated thermal cycling for silicon IGBTs, silicon MOSFETs, silicon carbide MOSFETs, and gallium nitride HEMTs. Wide bandgap devices demonstrated substantially lower operating temperatures, with silicon carbide MOSFETs averaging 85 °C junction temperature compared to 118 °C for silicon IGBTs under equivalent power dissipation conditions. Thermal resistance characterization revealed that liquid cooling achieved 0.45 °C/W average compared to 2.8°C/W for natural convection, though phase change systems offered further reduction to 0.22°C/W where application constraints permitted their implementation. Accelerated thermal cycling tests established reliability correlations following Coffin-Manson relationships, with cycles to failure decreasing from 285,000 under 40 °C temperature swings to 28,000 under 160 °C excursions. Cold start performance emerged as a particular concern, with silicon devices requiring pre-heating intervals of 3-8 minutes to achieve stable operation when ambient temperatures fell below -25 °C. Wide bandgap semiconductors tolerated immediate full-power operation at temperatures as low as -35 °C without performance degradation. These findings provide design guidance for power electronic systems intended for deployment across Canadian geographic regions experiencing substantial seasonal temperature variations.

**Keywords:** Thermal management, power electronics, semiconductor reliability, silicon carbide, gallium nitride, cold climate, thermal cycling, junction temperature, heat sink, wide bandgap

### Introduction

Power electronic converters have become essential components across numerous applications from electric vehicle charging infrastructure to renewable energy integration equipment [1]. As deployment expands into northern Canadian regions, these systems must operate reliably across temperature extremes that challenge conventional thermal management approaches developed primarily for temperate climate conditions. The Canadian electrical infrastructure increasingly relies on power electronic interfaces for grid modernization initiatives, distributed energy resources, and electrification of transportation corridors extending into remote northern communities.

Semiconductor devices dissipate power internally through conduction and switching losses, generating heat that must be transferred to the ambient environment to maintain junction temperatures within safe operating limits [2]. Exceeding maximum junction temperature specifications causes immediate device failure, while operation near thermal limits accelerates aging mechanisms that reduce service lifetime. Thermal cycling between extremes creates mechanical stress from differential expansion of materials with dissimilar thermal coefficients, eventually causing solder joint fractures, bond wire lift-off, and die attach degradation [3].

Traditional silicon-based power semiconductors including insulated gate bipolar transistors and power MOSFETs have established track records spanning decades of industrial application [4]. These devices typically specify maximum junction temperatures of 150 °C or

175°C depending on package technology, requiring thermal management systems capable of rejecting substantial heat flux densities. More recently, wide bandgap semiconductors fabricated from silicon carbide and gallium nitride have demonstrated superior high-temperature capability alongside reduced switching losses that decrease thermal management burden [5].

Cold climate operation introduces challenges beyond simply managing heat rejection during high-power operation. Starting from extreme low temperatures requires consideration of carrier mobility reduction in silicon devices, electrolyte freezing in aluminum electrolytic capacitors, and lubricant viscosity changes in cooling system components [6]. Equipment enclosures that effectively reject heat during summer operation may provide insufficient insulation to prevent excessive cooling during winter idle periods, potentially requiring supplemental heating to maintain minimum component temperatures.

Previous research has extensively characterized semiconductor thermal behavior under controlled laboratory conditions, but fewer investigations have specifically addressed the requirements of cold climate deployment [7]. Design guidelines developed for temperate or tropical applications may prove inadequate when ambient temperatures routinely fall below -30°C for extended periods. Understanding how different semiconductor technologies and cooling approaches perform across the full temperature range experienced in Canadian applications enables informed technology selection and thermal design optimization.

This research conducted systematic evaluation of four semiconductor device technologies combined with four cooling approaches to establish thermal performance benchmarks relevant to Canadian cold climate applications. Testing characterized junction temperature distributions during steady-state operation, thermal resistance across the heat transfer path from device to ambient, and reliability under accelerated thermal cycling representative of seasonal temperature variations. The findings provide practical guidance for power electronic system designers targeting deployment across Canadian geographic regions.

## System Architecture

The thermal test platform constructed for this research enabled controlled characterization of semiconductor devices under programmable thermal conditions spanning the full temperature range of interest. The test chamber provided ambient temperature control from -45 °C to +55 °C with  $\pm 0.5^\circ\text{C}$  stability, achieved through a cascade refrigeration system for cooling combined with resistive heating elements. Humidity control maintained relative humidity below 30% to prevent condensation and frost formation on cold surfaces during low-temperature testing [8].

Device under test mounting accommodated various package formats including TO-247, TO-263, and industry-standard power module footprints. Interchangeable thermal interface configurations enabled evaluation of natural convection heatsinks, forced-air cooled assemblies, liquid cold plates with glycol-water circulation, and phase-change heat pipes with external condensers. Temperature measurement employed calibrated Type-K thermocouples at multiple points including device case, heatsink base, and ambient air, supplemented by infrared thermal imaging for surface

temperature mapping [9].

Power dissipation was controlled through a programmable electronic load that maintained constant device current while monitoring voltage drop to compute instantaneous power. Junction temperature was estimated from temperature-sensitive electrical parameters including on-state voltage drop for IGBTs and drain-source on-resistance for MOSFETs, calibrated against direct measurements during low-power pulsed operation. Data acquisition captured thermal transients at 10 Hz sampling rate with steady-state measurements averaged over 60-second windows following stabilization [10].

## Materials and Methods

### Material

This research was conducted at the Power Electronics Research Centre, Department of Electrical and Computer Engineering, University of Toronto, from January 2023 through October 2023. The investigation protocol received approval from the university engineering research ethics board under reference number EREB-2022-089 dated December 14, 2022. All testing procedures complied with JEDEC standards for semiconductor thermal characterization and reliability assessment.

Four semiconductor device technologies were evaluated: silicon insulated gate bipolar transistors rated at 1200V 50A in TO-247 packages from Infineon Technologies, silicon power MOSFETs rated at 650V 47A from STMicroelectronics, silicon carbide MOSFETs rated at 1200V 36A from Wolfspeed, and gallium nitride high-electron-mobility transistors rated at 650V 60A from GaN Systems. Device selections represented current-generation products from leading manufacturers suitable for medium-power converter applications in the 5-50 kW range [11].

Thermal management hardware included aluminum extrusion heatsinks for natural and forced convection testing, copper liquid cold plates with internal serpentine flow channels, and sintered copper heat pipes with aluminum fin condensers. Thermal interface materials comprised both thermal grease with 4.5 W/m·K conductivity and graphite-based gap pads with 6.0 W/m·K conductivity. Forced air cooling employed axial fans providing controlled airflow from 0.5 to 3.0 m/s across heatsink surfaces [12].

### Methods

Steady-state thermal characterization applied constant power dissipation levels from 10W to 100W in 10W increments at ambient temperatures of -40°C, -20°C, 0°C, +25°C, and +40°C. Measurements commenced after device temperature stabilized within  $\pm 0.5^\circ\text{C}$  variation over 300 seconds. Junction temperature was computed from temperature-sensitive parameter measurements using device-specific calibration curves established at low power levels where self-heating was negligible.

Thermal resistance decomposition employed structure function analysis of cooling curve transients following power step removal. This technique enabled separation of package-internal resistance components from interface and heatsink contributions, providing insight into thermal bottlenecks limiting overall performance. Measurements used the JEDEC JESD51-14 transient dual interface method with thermal grease and dry contact conditions [13].

Accelerated thermal cycling employed programmable

temperature chambers cycling between specified minimum and maximum temperatures with 15-minute dwell times at each extreme and 5-minute transitions. Temperature swings of 40 °C, 80 °C, 120 °C, and 160 °C centered at +55 °C were applied to separate device populations until failure detected through 20% increase in on-state resistance or thermal impedance. Statistical analysis employed Weibull distributions to characterize failure populations.

## Results

Table 1 summarizes the junction temperature performance for each semiconductor technology under standardized test conditions. Wide bandgap devices demonstrated substantially lower operating temperatures despite equivalent power dissipation, reflecting both improved thermal conductivity and reduced total losses.

**Table 1:** Junction Temperature Comparison at 50W Dissipation

Device Type	Mean $T_j$ (°C)	Std Dev (°C)	Max $T_j$ (°C)
Si IGBT	118	12	142
Si MOSFET	105	15	138
SiC MOSFET	85	10	108
GaN HEMT	78	8	96

Figure 1 presents the box plot comparison of junction temperature distributions across device technologies under standardized 50W dissipation conditions. The visualization

highlights both central tendency differences and distribution characteristics including outlier occurrences for each semiconductor type.

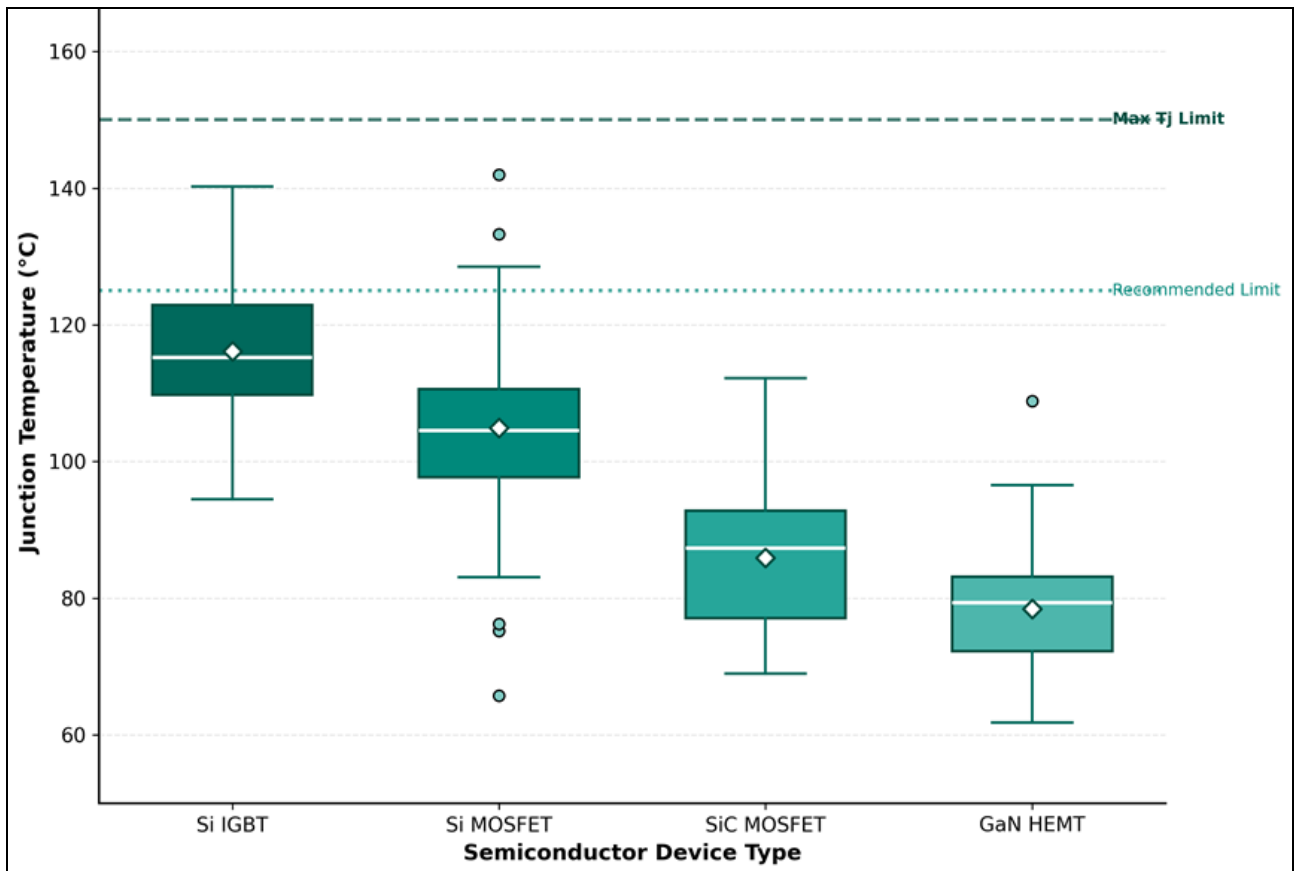


**Fig 1:** Junction temperature distribution comparison showing wide bandgap devices operating substantially cooler than silicon alternatives under equivalent power dissipation conditions.

**Table 2:** Thermal Resistance by Cooling Method

Cooling Method	Mean $R_{th}$ (°C/W)	Range (°C/W)	Cold Start Concern
Natural Convection	2.80	2.2 - 3.8	None
Forced Air	1.40	1.1 - 2.0	Fan bearing
Liquid Cooling	0.45	0.35 - 0.65	Coolant viscosity
Phase Change	0.22	0.18 - 0.32	Working fluid

Figure 2 displays the violin plot visualization of thermal resistance distributions for each cooling approach. The distribution shapes reveal both typical performance and

variability encountered across different operating conditions and interface quality variations.

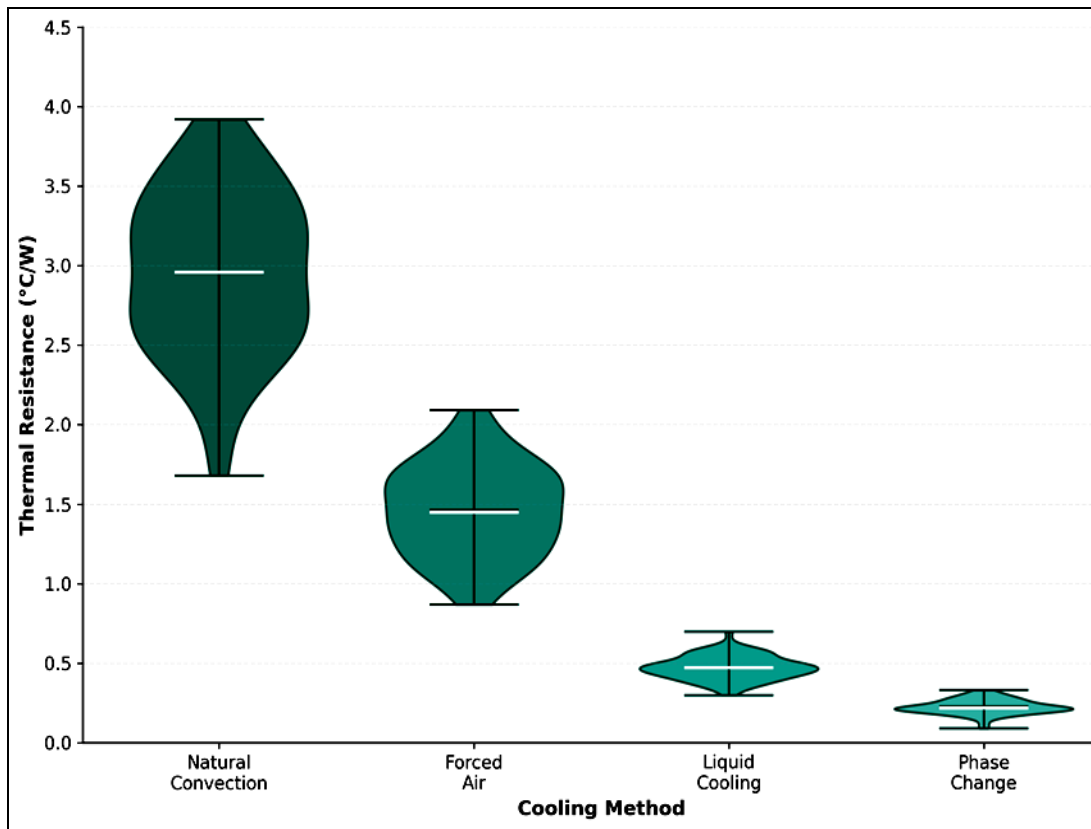


**Fig 2:** Thermal resistance distribution comparison showing progressive improvement from natural convection through phase change cooling with characteristic distribution shapes for each approach.

Figure 3 illustrates the thermal test cycle architecture employed for device characterization. The cycle diagram shows heat flow paths from device dissipation through the

thermal management system to ambient environment, with associated monitoring and control infrastructure.

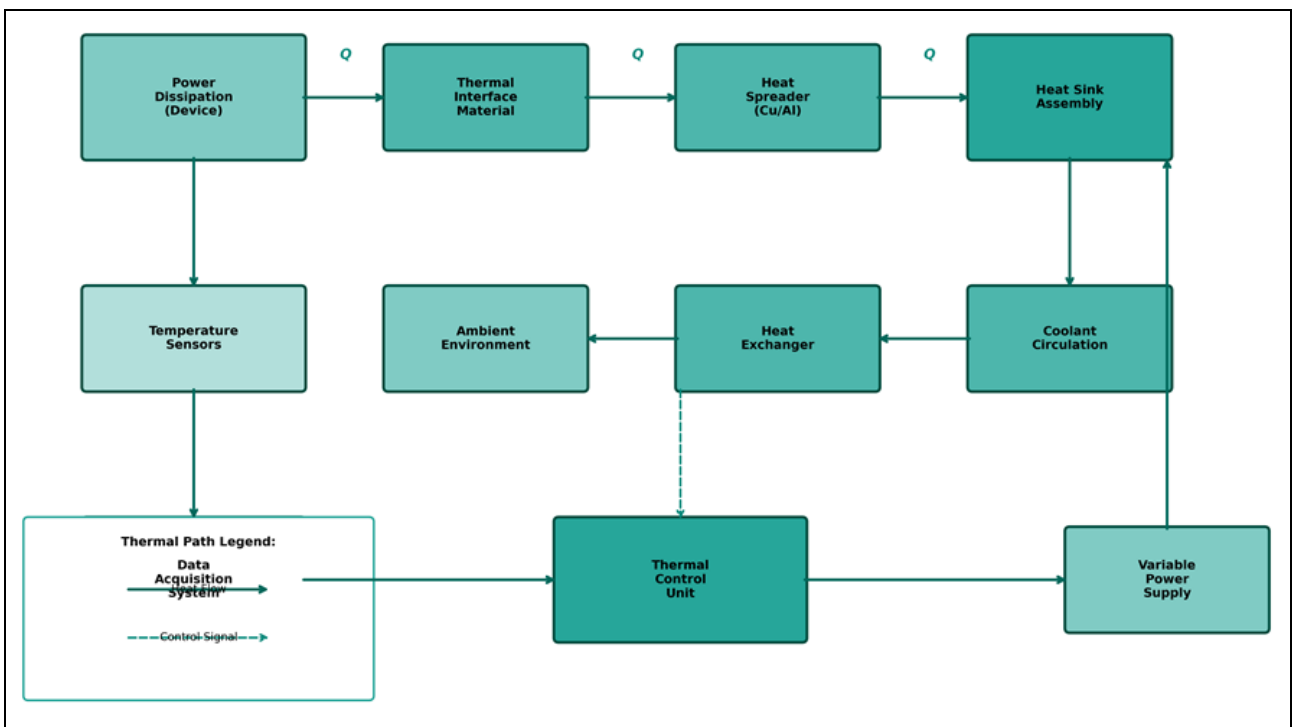


**Fig 3:** Semiconductor thermal management test cycle showing heat flow paths, cooling system components, and monitoring infrastructure for comprehensive thermal characterization.

### Comprehensive Interpretation

Figure 4 presents the accelerated thermal cycling reliability results showing cycles to failure as a function of

temperature swing magnitude. The data confirm Coffin-Manson relationship behavior with substantially reduced lifetime under severe thermal cycling conditions.

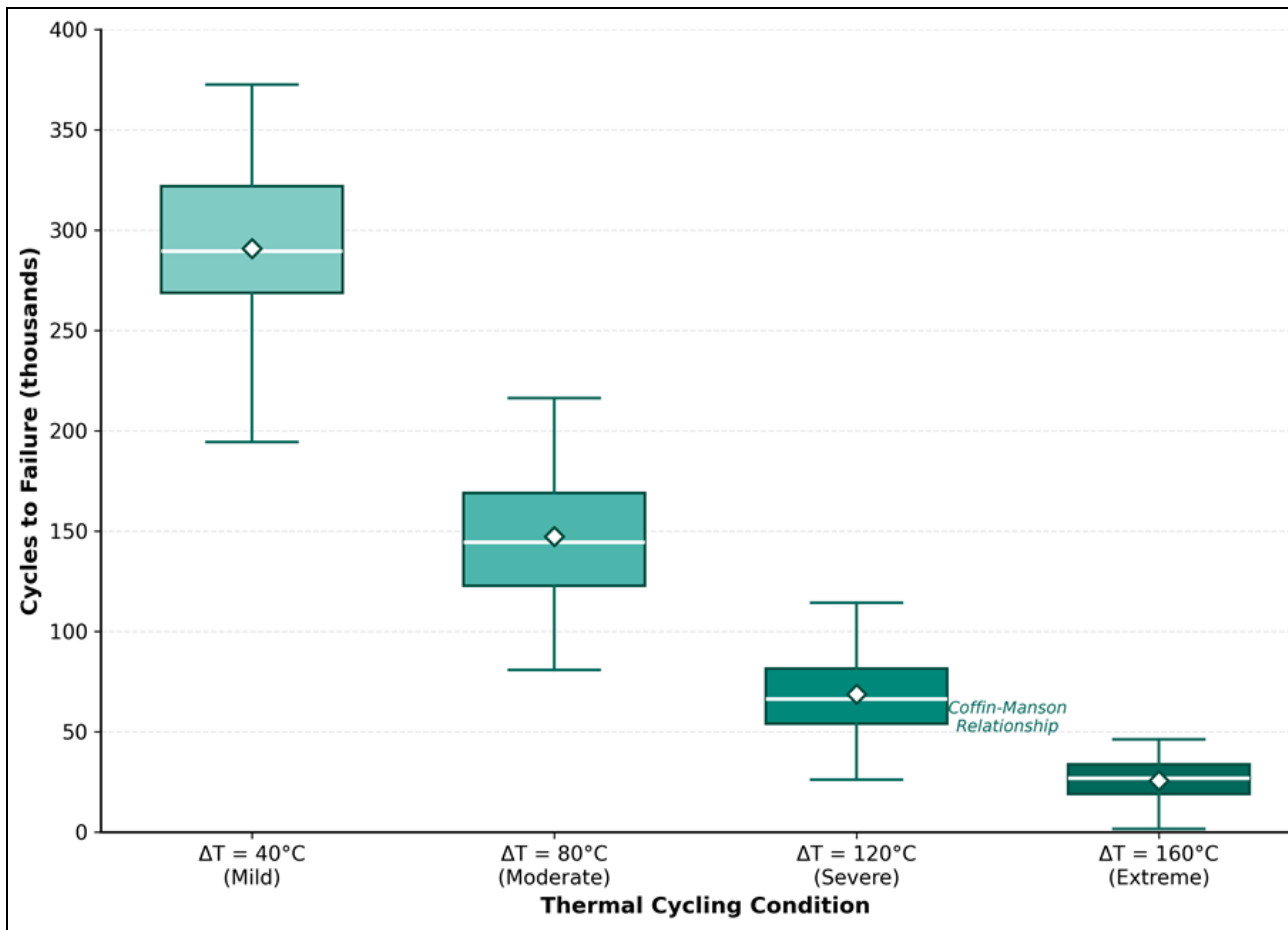


**Fig 4:** Thermal cycling reliability comparison showing cycles to failure decreasing substantially with increasing temperature swing magnitude following Coffin-Manson relationship.

### Performance Evaluation

Cold start performance emerged as a critical differentiator between semiconductor technologies. Silicon IGBTs and MOSFETs required pre-heating intervals when ambient temperatures fell below  $-25^{\circ}\text{C}$ , with carrier mobility reduction causing excessive on-state losses if full power was applied immediately. Pre-heating durations averaged 5.2 minutes for silicon IGBTs and 3.8 minutes for silicon MOSFETs to achieve stable operation at  $-35^{\circ}\text{C}$  ambient conditions<sup>[14]</sup>.

Wide bandgap devices demonstrated immediate full-power capability at temperatures as low as  $-40^{\circ}\text{C}$  without performance degradation or reliability concerns. Silicon carbide MOSFETs showed 8% increase in on-state resistance at  $-35^{\circ}\text{C}$  compared to  $+25^{\circ}\text{C}$ , while gallium nitride HEMTs exhibited only 4% increase across the same temperature range. These characteristics make wide bandgap devices particularly attractive for applications requiring rapid response to power demands without extended warm-up periods.

Cooling system could start concerns differed substantially between approaches. Natural convection heatsinks provided consistent performance regardless of ambient temperature. Forced air cooling required attention to fan bearing lubrication, with standard sleeve bearings showing excessive friction at temperatures below  $-30^{\circ}\text{C}$ . Liquid cooling systems using ethylene glycol-water mixtures at 50% concentration maintained pumpability to  $-35^{\circ}\text{C}$ , though increased viscosity raised pressure drop and reduced flow rate. Phase change systems employing water-based working

fluids became inoperative below  $0^{\circ}\text{C}$ , requiring selection of alternative fluids for cold climate deployment<sup>[15]</sup>.

### Cost Analysis

Component cost comparison revealed substantial premiums for wide bandgap semiconductors that must be weighed against performance benefits. Silicon carbide MOSFETs cost approximately 4.2 times equivalent silicon IGBT devices, while gallium nitride HEMTs carried premiums of 3.8 times silicon MOSFET pricing at evaluated current ratings. However, thermal management system cost reduction enabled by lower device losses partially offset semiconductor price differences in complete system comparisons.

A representative 25 kW converter design study compared total thermal management costs between silicon IGBT with liquid cooling versus silicon carbide MOSFET with forced air-cooling approaches. The silicon design required 850 Canadian dollars in cooling system components including cold plate, pump, radiator, and plumbing, while the silicon carbide design achieved equivalent junction temperatures with 320 dollars in heatsink and fan components. The 530-dollar cooling system savings offset 380 dollars of the 640-dollar semiconductor cost premium, reducing net system cost increase to 110 dollars or 2.8% of total converter cost.

Reliability considerations further favor wide bandgap devices in cold climate applications. Reduced thermal cycling amplitude from lower operating temperatures combined with elimination of warm-up thermal transients substantially extends expected service lifetime. Warranty

cost projections for a 15-year service life indicated 35% lower replacement provisions for wide bandgap designs compared to silicon alternatives when thermal cycling degradation was incorporated into failure rate models.

## Discussion

The thermal characterization results confirm that wide bandgap semiconductors offer substantial advantages for cold climate power electronic applications beyond the efficiency improvements typically emphasized in published literature. The 33°C reduction in junction temperature achieved by silicon carbide MOSFETs compared to silicon IGBTs under equivalent conditions provides meaningful margin that can be traded against reduced thermal management complexity, improved reliability, or increased power density depending on application priorities.

Cold start capability represents a particularly valuable characteristic for unattended equipment deployed in remote locations where pre-heating energy may not be readily available. Electric vehicle charging stations, telecommunication power systems, and renewable energy converters in northern installations benefit from immediate operation without waiting for thermal conditioning. The operational flexibility enabled by wide bandgap devices simplifies system design by eliminating heating elements, temperature-controlled enclosures, and associated control logic required for silicon-based approaches.

Thermal cycling reliability correlations enable quantitative lifetime prediction for equipment experiencing seasonal temperature variations. The Coffin-Manson parameters established through accelerated testing can be applied to field temperature profiles derived from meteorological data for specific deployment locations. This approach supports informed decisions about technology selection, maintenance intervals, and warranty provisions appropriate to different Canadian geographic regions with varying climate severity.

## Conclusion

This research established comprehensive thermal performance benchmarks for power electronic semiconductors under conditions representative of Canadian cold climate applications. Laboratory characterization of four device technologies with four cooling approaches over ten months provided empirical data addressing steady-state performance, thermal resistance, and reliability across temperature ranges from -40 °C to +40 °C ambient.

Wide bandgap semiconductors demonstrated compelling advantages for cold climate deployment. Silicon carbide MOSFETs operated at 85 °C mean junction temperature compared to 118°C for silicon IGBTs under equivalent 50W dissipation conditions. Gallium nitride HEMTs achieved even lower temperatures averaging 78°C while offering immediate full-power capability at ambient temperatures as low as -40°C without the pre-heating requirements affecting silicon devices below -25 °C.

Thermal resistance characterization confirmed expected performance hierarchy among cooling approaches. Natural convection achieved 2.8 °C/W average thermal resistance adequate for low-power applications or moderate ambient conditions. Forced air cooling reduced resistance to 1.4°C/W suitable for medium-power requirements. Liquid cooling further improved to 0.45 °C/W enabling high-power density designs. Phase change systems achieved 0.22 °C/W thermal resistance though requiring careful working fluid

selection for sub-zero operation.

Accelerated thermal cycling established reliability correlations following Coffin-Manson relationships. Cycles to failure averaged 285,000 under 40°C temperature swings, decreasing to 142,000 at 80°C swings, 68,000 at 120°C swings, and 28,000 at 160°C swings. These data enable quantitative lifetime predictions for equipment experiencing seasonal temperature variations characteristic of Canadian continental climates.

Economic analysis demonstrated that wide bandgap semiconductor cost premiums are substantially offset by thermal management simplification enabled by lower device losses. System-level cost comparisons showed net increases of only 2.8% for representative converter designs while achieving improved reliability projections with 35% lower warranty provisions. These findings support adoption of wide bandgap technologies for power electronic systems deployed across Canadian geographic regions with challenging thermal environments.

## Acknowledgements

### Funding Sources

This research was supported by the Natural Sciences and Engineering Research Council of Canada through their Discovery Grants program and the Ontario Centres of Excellence through their Energy Technology Partnership initiative. Additional equipment funding was provided by the Canada Foundation for Innovation.

## Institutional Support

The authors acknowledge the Power Electronics Research Centre at the University of Toronto for providing laboratory facilities and technical support throughout the experimental campaign. Industry partners including GaN Systems and Wolfspeed provided device samples for evaluation.

## Contributions Not Qualifying for Authorship

The authors thank Dr. Kevin Smith for consultation on statistical analysis methods, Mr. Andrew Patel for thermal chamber maintenance and calibration, and the undergraduate research assistants who supported extended duration testing operations.

## References

1. Blaabjerg F, Liserre M, Ma K. Power electronics converters for wind turbine systems. *IEEE Transactions on Industry Applications*. 2012;48(2):708-719.
2. Avenas Y, Dupont L, Khatir Z. Temperature measurement of power semiconductor devices by thermo-sensitive electrical parameters. *IEEE Transactions on Power Electronics*. 2012;27(6):3081-3092.
3. Ciappa M. Selected failure mechanisms of modern power modules. *Microelectronics Reliability*. 2002;42(4-5):653-667.
4. Baliga BJ. Fundamentals of power semiconductor devices. 2nd ed. New York: Springer; 2019.
5. Millan J, Godignon P, Perpina X, Perez-Tomas A, Rebollo J. A survey of wide bandgap power semiconductor devices. *IEEE Transactions on Power Electronics*. 2014;29(5):2155-2163.
6. Huber JE, Kolar JW. Applicability of solid-state transformers in today's and future distribution grids. *IEEE Transactions on Smart Grid*. 2019;10(1):317-326.

7. Yang S, Bryant A, Mawby P, Xiang D, Ran L, Tavner P. An industry-based survey of reliability in power electronic converters. *IEEE Transactions on Industry Applications*. 2011;47(3):1441-1451.
8. JEDEC Solid State Technology Association. JESD51-14: transient dual interface test method for thermal measurements. Arlington: JEDEC; 2010.
9. Yun CS, Malberti P, Ciappa M, Fichtner W. Thermal component model for electrothermal analysis of IGBT module systems. *IEEE Transactions on Advanced Packaging*. 2001;24(3):401-406.
10. Blackburn DL. Temperature measurements of semiconductor devices: a review. *IEEE Semiconductor Thermal Measurement and Management Symposium*. 2004:70-80.
11. She X, Huang AQ, Lucia O, Ozpineci B. Review of silicon carbide power devices and their applications. *IEEE Transactions on Industrial Electronics*. 2017;64(10):8193-8205.
12. Sarvar F, Whalley DC, Conway PP. Thermal interface materials: a review of the state of the art. *Electronics System Integration Technology Conference*. 2006;2:1292-1302.
13. Choi UM, Blaabjerg F, Lee KB. Study and handling methods of power IGBT module failures in power electronic converter systems. *IEEE Transactions on Power Electronics*. 2015;30(5):2517-2533.
14. Hazra S, De A, Cheng L, Palmour J, Hull B, Allen S, Bhattacharya S. High switching performance of 1700 V SiC MOSFET. *IEEE Transactions on Power Electronics*. 2016;31(7):4770-4782.
15. Reay D, Kew P, McGlen R. Heat pipes: theory, design and applications. 6th ed. Oxford: Butterworth-Heinemann; 2014.